JOURNAL OF MATERIALS SCIENCE **35** (2000) 4079–4086

Ion nitriding of a sintered iron molybdenum alloy

M. R. PINASCO
Department of Chemistry and Industrial Chemistry, University of Genoa, Genoa, Italy
E-mail: metal@chimica.unige.it

M. G. IENCO
Department of Chemistry and Industrial Chemistry, University of Genoa, Genoa, Italy

P. GUARNONE
Ansaldo Ricerche, Genoa, Italy

G. F. BOCCHINI
PM consultant

The behaviour of a sintered alloy Fe Mo 1.5 C 0.01 in two density states when subjected to an ion nitriding process is analysed. The thermochemical treatment was carried out with three different combinations of parameters (time, nitriding atmosphere). The analyses of the material after treatment included dimensional measurements, macro- and micro hardness determinations, diffractometric analysis and microstructural examination with an optical microscope and a scanning electron microscope equipped with an EDX system. All treatments led to satisfactory results for the material in the two density states: the volume mass is not a discriminative parameter in this case.

1. Introduction

The need for producing mechanical components with close dimensional tolerances at low costs has led the development of powder metallurgy technologies. At the same time there is also a demand for good surface characteristics (resistance to wear, corrosion etc.) and consequently a surface treatment is required in order to increase the material hardness. Among the different surface treatments ion nitriding is one of the most effective. It is known that in bulk steels Mo, as an alloying element, improves the hardenability. The same effect also exists for powder metallurgy steels. In addition Mo does not have a negative effect on the sintering parameters.

In 1990 a new iron prealloyed powder Astaloy Mo with 1.5 % Mo was introduced by Höganas, and in the same period in the USA a new powder with 0.85% Mo was commercialised. Both powders did not present significant differences in compressibility with respect to atomised Fe powder but they showed a considerable improvement in hardenability [1–3]. Mo sintered steels are a good choice if a suitable surface treatment is adopted [4–6]. Ion nitriding is one of the suitable treatments.

Ion nitriding is a relatively new process and its mechanism is not yet completely understood [7]. It seems that atomic nitrogen reacts with perfectly cleaned metallic surfaces, and then the reaction nitrogen diffuses towards the inner part of the material. Together with nitrogen different gaseous species also can react in the same manner. The process is carried out inside a vacuum chamber and a plasma is created with an highly intensified tension electric discharge inside the gas. Nitrogen ions accelerated by an electric field strike against the metallic surface and react with the metal itself. The process is similar to ionic bombardment. The vacuum chamber acts as the anode while the components to be treated are the cathodes.

Typical process parameters are:

low pressure (up to 1.3 MPa)
high DC voltyage (200 to 1000 V)
low current density (generally <10 mA/cm2)
relatively low temperature (375 to 650°C).

An accurate cleaning process (normally hydrogen bombardment) is required before nitriding in order to remove any contamination from the surface. This step of the treatment is very critical when the components to be nitrided are sintered parts. In fact impurities could be trapped inside pores during the sintering process and could be release later on during the nitriding process.

Main advantages of ion nitriding include: composition control and nitrided layer uniformity, low component distortion, good thickness uniformity, lower process temperature, lower power consumption, possibility of process automation, and possibility of protection for the areas that are not to be nitrided. For use with powder metallurgy there is another great advantage: the penetration of gases inside pores is (theoretically) avoided so that the risk of core brittleness decreases.

Recent studies [8, 9] showed that process improvements can be reached with an increased glow discharge. Together with the conventional discharge an auxiliary electron source and a positive electrode are used. Extra electrons emitted by the filament due to the thermionic effect are accelerated towards the positive electrode and

strike against molecules, atoms and gas ions. This process is carried out at lower pressure (<13 Pa) than the conventional one and is characterised by an high ionisation rate with an increased impact power of plasma.

References about ion nitriding on sintered components are few and nothing has been done until now about ion nitriding at low pressure.

2. Materials and methodologies

The sintered material studied is a Fe - Mo alloy commercially known as Astaloy Mo. This alloy is produced from a completely alloyed water atomised powder with the aim of testing surface treatments on it. The samples are cylinders 25 mm in diameter and 25 mm long produced in two different density states. Samples were prepared according to a normal industrial production procedure.

The nominal alloy composition is:

$$\mathrm{Fe; Mo} = 1.5\%, \mathrm{C} < 0.01\%.$$

Hereinafter the two different density conditions will be identified by the letters A and B. Alloy A was pressed at 590 MPa, pre-sintered at 850°C for 20 minutes in 90% N2 10% H2, then pressed at 785 MPa and re-sintered at 1120°C for 30 minutes in 90% N2 10% H2. Alloy B was pressed at 590 MPa and sintered at 1120°C for 30 minutes in 90% N2 10% H2. Both materials were ion nitrided at 590°C by a German company with three distinct process parameters (Table I).

The materials in the as sintered conditions were examined using different techniques:

- Dimensional measurements (with a centesimal micrometer), weight measurements and calculation of volume mass.
- Vickers and Brinell hardness measurements on as received surfaces.
- Optical and Scanning Electron Microscopy.
- Hg porosimetry in order to measure pores size and distribution.
- Porosity measurement by image analysis, formula, reticule.
- X ray diffractometry.

After nitriding the materials were analysed by:

- Dimensional measurements.
- Vickers Hardness (HV5, HV1) on the nitrided surface.
- microhardness profiles (HV0.05) along the cross section.
- Optical and Scanning Electron Microscopy with EDX
- X-ray diffractometry.

TABLE I Ion nitriding parameters at 590°C

Treatment	N2%	H2%	CH4%	*t* (h)
1	25	75	-	8
2	25	75	-	24
3	75	25	traces	24

TABLE II Volume mass, HV5 and HB62.5 hardness values of materials A and B

	VOLUME MASS (10^3 kg/m^3)				
	min	**mean**	max	HV5	HB62.5
MATERIAL A	7.4	**7.49**	7.5	106 ± 10	114 ± 4
MATERIAL B	6.8	**6.96**	7.0	94 ± 10	87 ± 5

3. Experimental results

3.1. Base material

Table II shows the volume mass and hardness values of the material in the two density states. Hardness values are indicated according to the traditional scales.

The volume mass of material B is very close to that reported by Remges and Zimmerman [10] as the threshold under which it is not possible to obtain satisfactory results. Otherwise the process parameters used in that study were quite different from ours.

The hardness measurements seem to depend on the porosity amount and this may be explained as follows:

For loads higher than 5 kg it is possible to define a "normal" or "apparent" hardness that depends on the metal structure and porosity level.

For loads between 3 and 0.2 kg the influence of porosity on hardness decreases without reaching the zero level.

For loads lower than 0.1 kg the influence of porosity is negligible (some differences could be observed when the operator changes).

Hardness was measured with HV5 and HB62.5 scales. The mean value was obtained from 30 measurements, the minimum required for a statistical approach. According to the deegre of value scattering, the HV5 scale seems to be less effective than the HB62.5 scale to measure the hardness of this material [11].

The differences between results may be explained by the smaller area subjected to the test when the load is low. If there is a porosity non uniformity due to production defects this will be revealed better with lower loads, and the scatter of the results obtained will be greater. The more dense alloy shows values only a little higher than the less dense alloy, this is due to the slight effect of double pressing on the surface density.

Different analysis techniques (image analysis, formula $p = 1 - d/D$ where d is the volume mass of the sintered material and D is the corresponding volumic mass of the bulk material, reticule technique (Montecarlo) on micrographs) led to coherent porosity values: 4.3% for material A and 11.4% for material B.

Fig. 1 shows the pore size distribution obtained with a Hg porosimeter for materials A and B. The considerable difference between materials shown by the graphs is confirmed by microstructural analysis on the as polished samples.

Pores in material B have an irregular shape and this is an indication of interconnected porosity. The pores in material A instead have a regular circular shape and, accordingly, the presence of interconnected porosity can

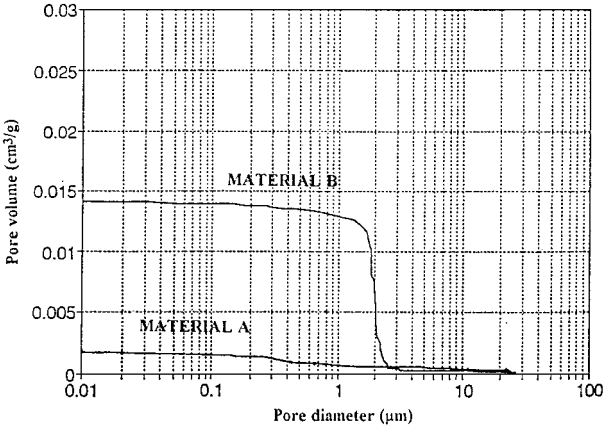

Figure 1 Distribution diagram of surface pore dimensions for materials A and B.

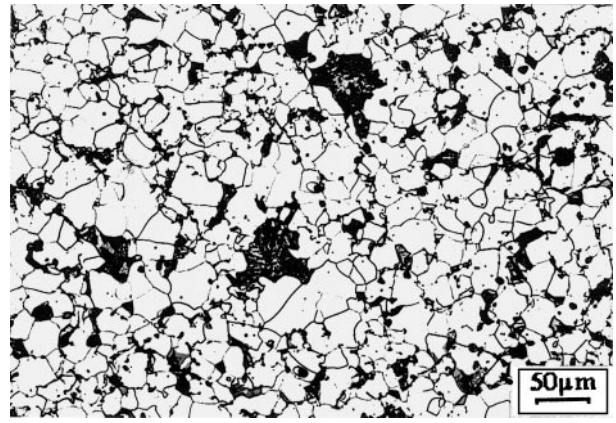

Figure 3 Material A: ferrite structure with granulare bainite islands (Nital 2% etching).

be excluded (Fig. 2a and b). The relationship between density and pore morphology is of the same kind as that observed for pure sintered Fe obtained from atomised powder. This confirms that the presence of 1.5 % Mo does not influence the relationships between volume mass and porosity.

Metallographic etching 2% with Nital revealed that the structure is almost completely polygonal ferrite (Fig. 3). The presence of granular bainite is sometimes observed but its distribution is different depending on sample and zone of the same sample. A small amount of residual austenite was found. very close to the bainite islands (Fig. 4). The presence of these phases is attributable to an irregular distribution of carbon probably derived from the organic lubricant used during the sintering process. Another influencing factor is the large cooling gradient in the oven where sintering was carried out.

EDX analysis showed (within the limits of the technique) an homogeneous Mo distribution.

3.2. Material after nitriding

The examination of the nitrided surfaces showed a uniform roughness with some irregularities corresponding to disuniformity in the substrate (probably residual porosity). (Fig. 5).

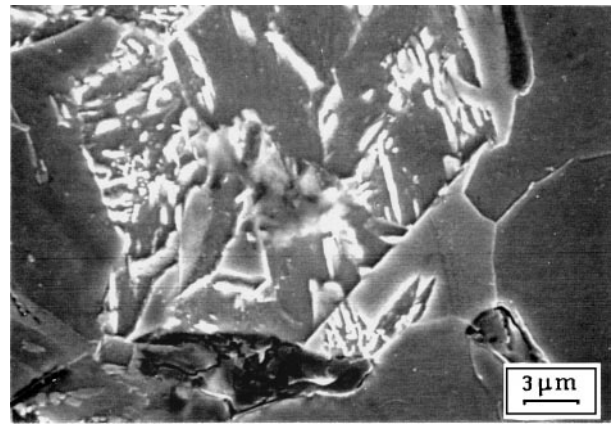

Figure 4 Residual austenite adjoining the bainite (SEM).

3.2.1. Dimensional changes and Vickers hardness

The per cent increase in diameter of the samples after the nitriding treatments is reported in Table III. The limit of dimensional changes due to the treatment admitted for this kind of material is 0.12% because a higher variation implies the risk of brittleness.

All values for the materials studied are under the limit. Material B shows higher values than material A. The diffusion of nitrogen inside the core is limited and consequently the material toughness should still be

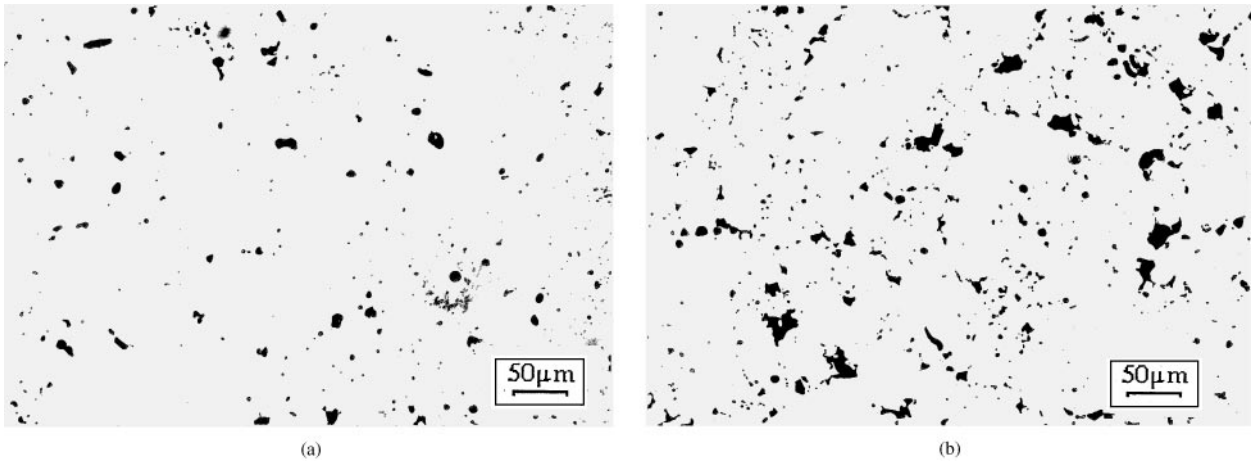

Figure 2 Porosity features: (a) material A; (b) material B.

TABLE III Per cent dimensional variations

	$\Delta\phi$ %	
TREATMENT	MATERIAL A	MATERIAL B
1	0.04	0.12
2	0.04	0.08
3	0.04	0.12

TABLE IV HV1 and HV5 hardness values after the nitriding treatments

		HV5			HV1		
Material	Treatment	min.	mean	max	min.	mean	max
A	1	197	**251**	327	285	**318**	355
A	2	163	**274**	358	378	**412**	448
A	3	202	**325**	453	342	**382**	422
B	1	109	**129**	151	219	**248**	263
B	2	125	**164**	237	219	**249**	290
B	3	131	**165**	179	235	**248**	261

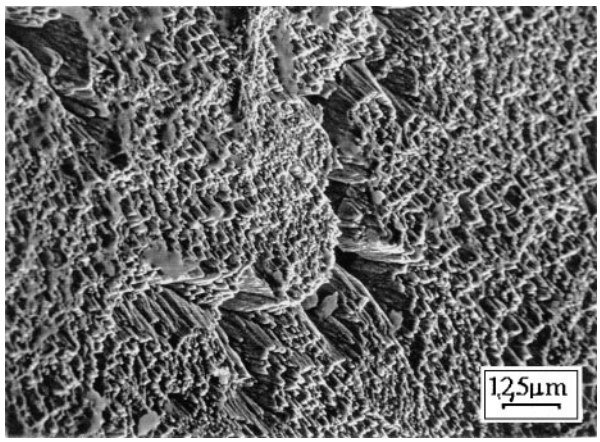

Figure 5 Typical feature of a nitrided surface.

good. Vickers macro-hardness tests were carried out with 1 kg and 5 kg loads; microhardness profiles along the cross section were obtained with a 0.01 kg load.

Table IV reports the macro-hardness results (mean, minimum and maximum value). Values obtained with the lower load are higher and less scattered due to the fact that the area affected by the test is confined to the nitrided layer. Regarding the 5 kg test the surface hardness differences after nitriding are correlated to the differences before nitriding for the two materials.

The hardness increase due to the nitriding treatment is more evident in material A (150–230 with 5 kg, 200–300 with 1 kg) than in material B (20–60 with 5 kg, 150 with 1 kg). The structure of the nitrided layer is similar in the two materials, but material B shows an increase in pore dimensions under the layer, a phenomenon that was not observed in material A. No references exist that report this phenomenon. A possible explanation is that a too high nitrogen concentration can induce material brittleness. The embrittled material can detach later on during metallographic preparation or can break during the hardness test.

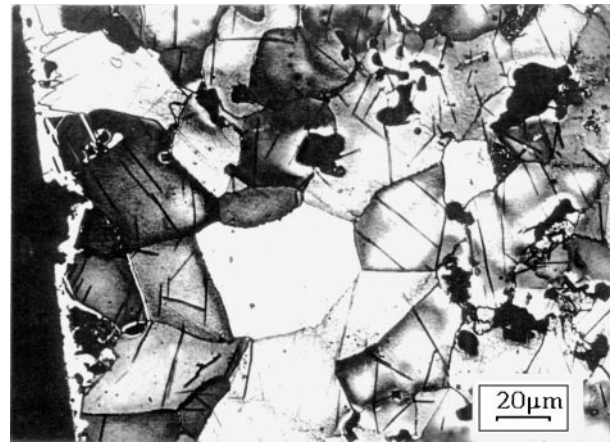

Figure 6 Material A after treatment 1: surface layers (Nital 2% etching).

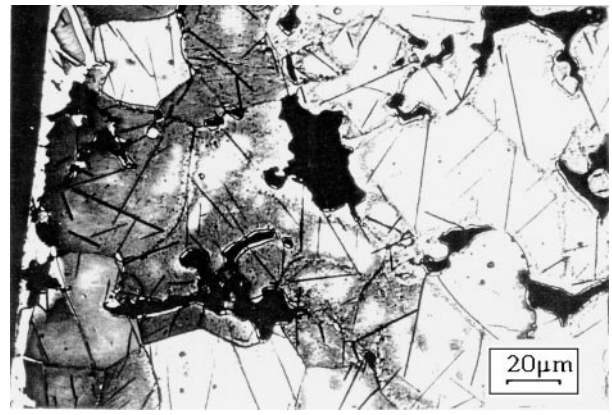

Figure 7 Material B after treatment 1: surface layers (Nital 2% etching).

3.2.2. Microstructural analysis

Treatment 1. Microstructural examination of the as polished samples showed that in material B the increase in pore dimensions is present up to a depth of 800 μm. The microstructure of the nitrided layers (Figs 6 and 7), evident after Nital etching, is similar for the two materials. The white layer is very thin and with irregular thickness (3–8 μm in material A, 2–12 μm in material B, Table V). In material B the compound layer has a certain grade of infiltration and a reticular shape. The thickness of the diffusion layer is about 250 μm for both materials. In material A the ferrite rich in nitrogen is present together with points where there is only diffusion at grain boundaries; in material B the diffusion at grain boundaries starts just under the azoferrite zone. In the diffusion layer there is also the presence of needle shaped nitrides grown along preferential directions towards the grain centre. The amount of nitrides is superior in material B. In this material at the diffusion layer/core interface zone there is also a continous precipitation of fine nitrides just visible with the optical microscope (Fig. 8). In the diffusion layer there are also a few, small islands of braunite.

Treatment 2. Material B after treatment 2 shows an increase in pore dimensions up to a depth of 700 μm. In material A the different zones of the diffusion layer are well defined contrary to material B (Figs 9 and 10). The mean thickness of the white layer is larger than in the previous treatment and is extremely

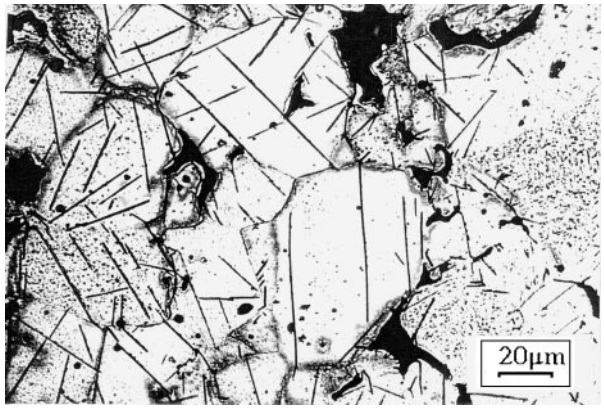

Figure 8 Material B after treatment 1: nitrides of very small dimensions in the interior of the nitrided zone.

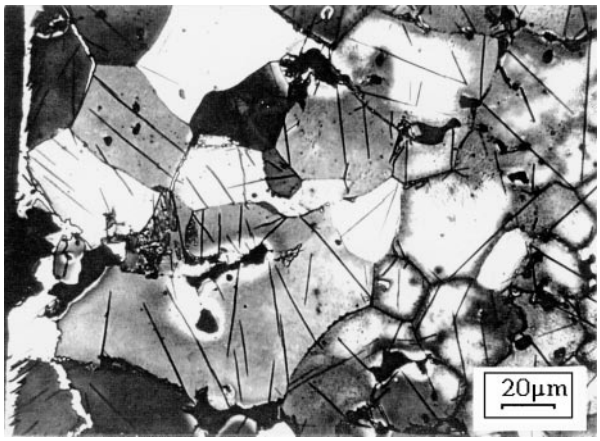

Figure 9 Material A after treatment 2: surface layers (Nital 2% etching).

Figure 10 Material B after treatment 2: surface layers (Nital 2% etching).

variable (2.5–13 μm for material A, 3.5–16 μm for material B). The diffusion layer in material A is about 350 μm and is composed by a layer of azoferrite and nitrides and another layer with only grain boundary diffusion. The final layer is constituted only by nitrides in ferrite. Material B has a diffusion layer of about 400 μm. At the same depth it is possible to find together azoferrite grains (mainly towards the surface and around pores) and diffusion zones only along grain boundaries. In some grains there is the continous precipitation of small nitrides; the zone of nitrides in ferrite grains is absent. Both materials show braunite islands in the diffusion layer.

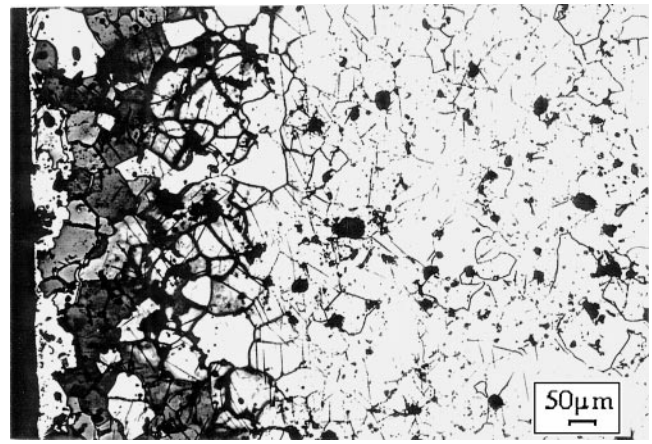

Figure 11 Material A after treatment 3: surface layers (Nital 2% etching).

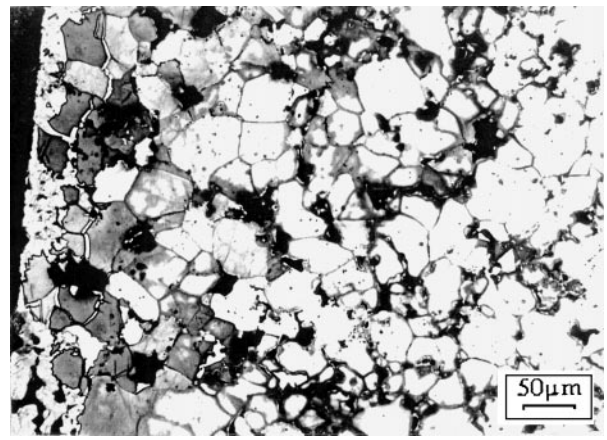

Figure 12 Material B after treatment 3: surface layers (Nital 2% etching).

Treatment 3. The microstructural aspect of materials A and B is the same after treatment 3. The different layers however have different thicknesses and dispositions (Figs 11 and 12). Material A has a white layer variable between 2 and 27 μm that has a tendency to infiltrate through the azoferrite grains below. The diffusion zone of about 200 μm shows a well defined disposition of layers. The surface layer is constituted by azoferrite and needle-shaped nitrides followed by a grain boundary diffusion zone and finally by nitrides in a ferrite zone. Braunite islands are also present.

The observation of material B as polished shows the phenomenon of pore enlargement for more than 1 mm in depth. The white layer varies between 12 and 46 μm, has an irregular shape and penetrates around the azoferrite grains to form a reticule. The diffusion layer is very thick (>500 μm) and sometimes there are preferential diffusion paths that lead to higher thickness. It is constituted by an external layer of azoferrite richin nitrogen and by an internal layer where azoferrite (near large pores) and grain boundary diffusion coexist. Few and thin nitrides are present. There is not a layer where only needle-shaped nitrides are present.

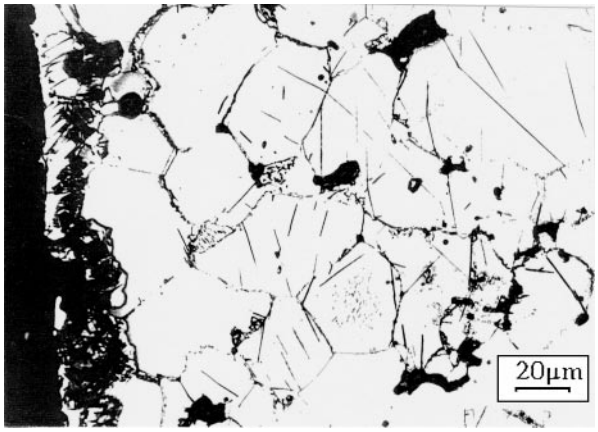

Figure 13 Material B after treatment 3: the black phase in the compound layer is ε carbonitride (Murakami etching).

3.2.3. XRD analyses

XRD analyses showed the exclusive presence of γ' phase in the samples subjected to treatments 1 and 2. In both materials subjected to treatment 3 ($N_2 : H_2 = 75 : 25$ with traces of CH_4) a small amount of ε phase containing C was also found. The presence of C in the material or of CH_4 in the nitriding atmosphere promotes the formation of the ε phase [5].

Other studies report that when bulk iron is gas nitrided the ε phase could be localised not only in the inner part of the white layer but also in both the inner and outer zone, while when steels are gas nitrided the ε phase is mixed with the γ' phase [12–14].

Murakami's etchant (selective towards ε phase containing C) [12] was used to distinguish carbonitride inside the compound layer (Fig. 13). Carbonitride was

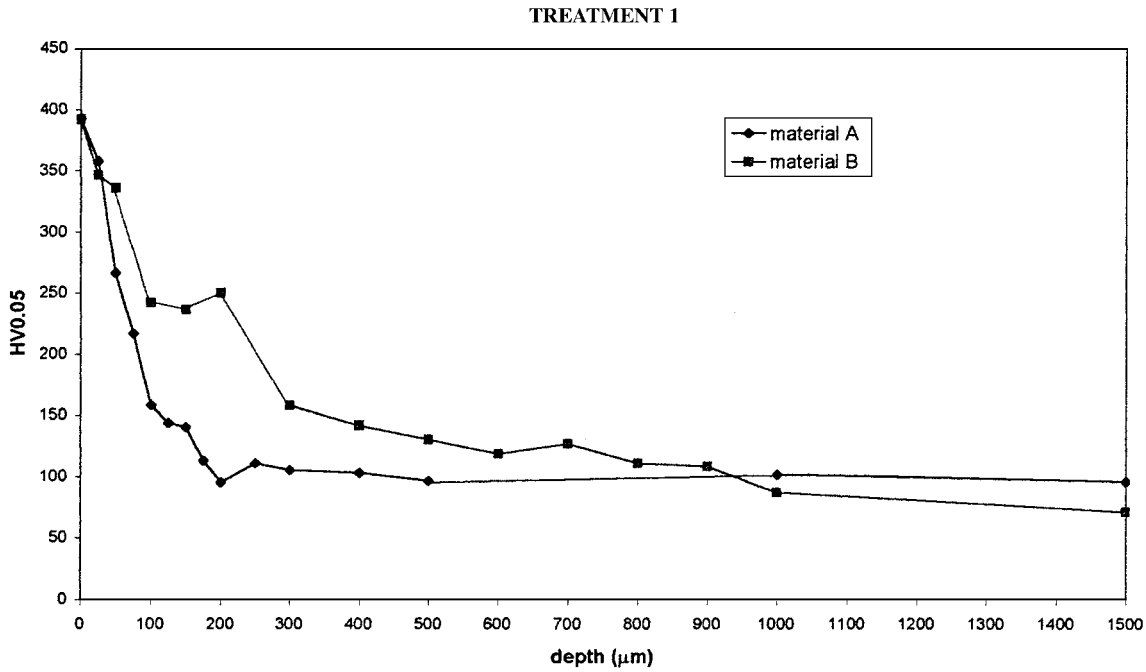

Figure 14 Microhardness profiles of materials A and B after treatment 1.

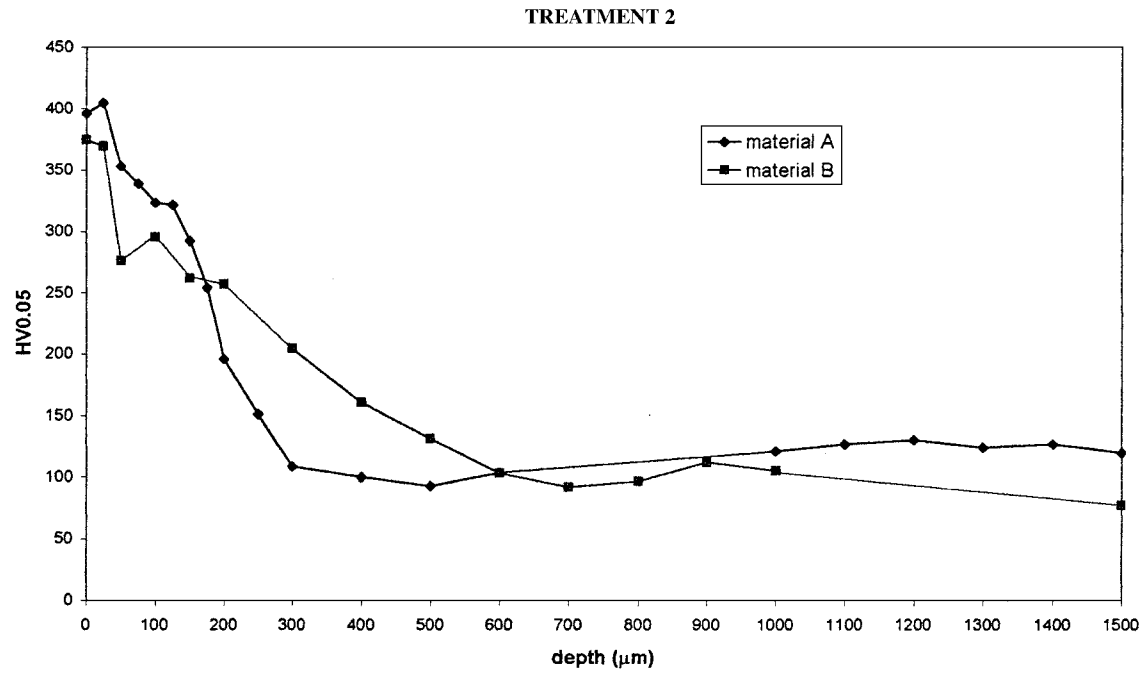

Figure 15 Microhardness profiles of materials A and B after treatment 2.

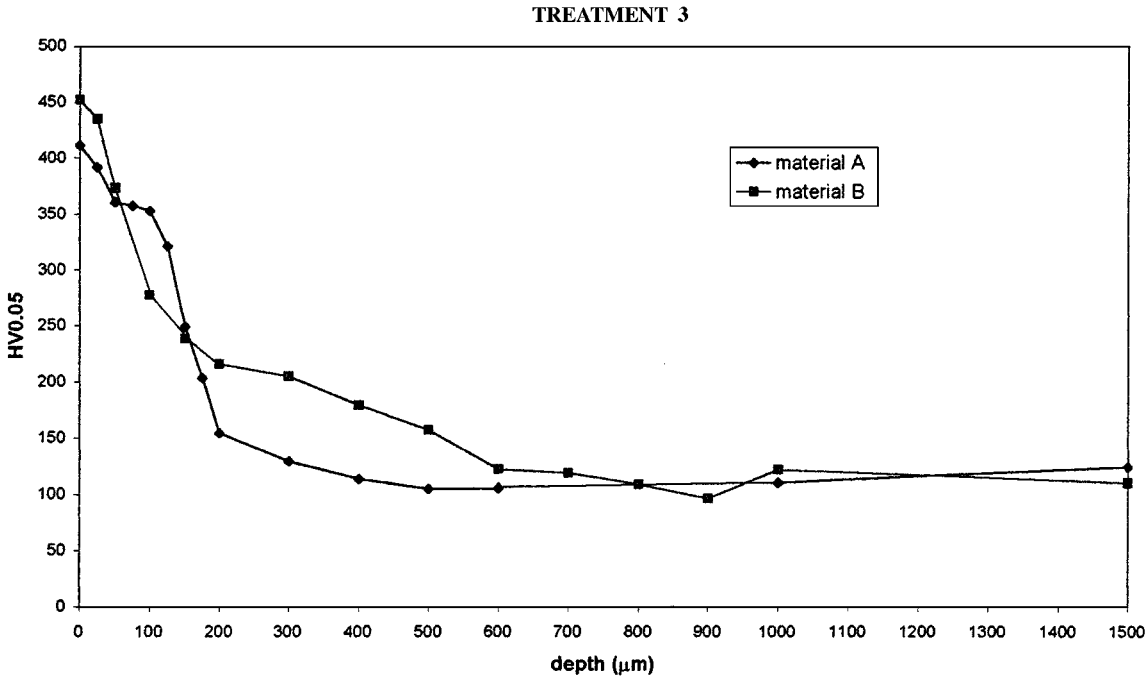

Figure 16 Microhardness profiles of materials A and B after treatment 3.

identified in the internal part of the white layer at the boundary with the substrate [12, 13]. Carbonitride is present in smaller amounts in material A than in B. In this case the carbon source was CH_4 from the gas atmosphere.

3.2.4. Microhardness profiles

Because of the as delivered material characteristics the hardened layer is very irregular, and in order to obtain reliable microhardness profiles as a function of the distance from the surface, several set of measurements were necessary (Figs 14–16).

Table VI reports the main values for each profile: maximum hardness value, distance *d* from the surface at which the curve reaches a plateau and nitriding depth dN at which the hardness has the mean value between the maximum and the plateau. The maximum hardness values depend slightly on the nitriding times and atmospheres. All maximum values are comparable except those for material B after treatment 3, which are higher due to the presence of ε phase in the compound layer. The increase in nitriding time leads to a small increase in hardness (after treatment 2 only a little higher than after treatment 1). The plateau value of material B is higher than for material A due to the large amount of porosity.

4. Discussion

The experimental results show that in the case of ion nitriding the volume mass of the material is not a discriminative parameter especially in atmospheres without C. This observation is in agreement with previous studies [15]. However the volume mass does influence the characteristics of the nitrided layers.

Regarding the compound layer it was observed that it is more irregular and thicker in the less dense material.

TABLE V Thickness of the nitrided layers

	TREATMENT 1		TREATMENT 2		TREATMENT 3	
	compound layer (μm)	diffusion layer (μm)*	compound layer (μm)	diffusion layer (μm)*	compound layer (μm)	diffusion layer (μm)*
MATERIAL A	3 ÷ 8	250	2.5 ÷ 13	300	2-27	200
MATERIAL B	2 ÷ 12	250	3.5 ÷ 16	450	12-46	>500

*without the layer where only nitrides are present.

TABLE VI Main parameters of microhardness profiles

	TREATMENT 1			TREATMENT 2			TREATMENT 3		
	HV0.05 max	*d* (mm)	d_N (mm)	HV0.05 max	*d* (mm)	d_N (mm)	HV0.05 max	*d* (mm)	d_N (mm)
MATERIAL A	390	0.3	0.07	404	0.4	0.18	408	0.3	0.16
MATERIAL B	374	1.0	0.12	384	0.7	0.26	450	0.7	0.12

The structural differences are particularly evident after treatment 3: the boundaries of this layer are not clearly defined.

Both materials show, after the nitriding treatments, the nucleation of needle shaped nitrides inside the diffusion layer. These nitrides grow with a crystallographic orientation related to that of the grain from which they arise. Some nitrides are in the external part of the diffusion layer and have large dimensions; indicating that they were nucleated at the treatment temperature in points where nitrogen was abundant. Other nitrides smaller than the previous ones present in the internal layer of the diffusion zone precipitate during cooling due to the diminished solubility of N in Fe [16].

In the less dense material after treatments 1 and 2 there is continous precipitation of very small nitrides that have a different morphology than the γ' phase [16]. According to other authors [12], this may be the tetragonal α'' phase. In all cases the nitriding treatment increased the difference in hardness HV1 and HV5 between materials A and B. This factor is not due to differences in microstructural aspects but rather to the enlargement of pore dimensions in material B.

If a comparison of the microhardness profiles is made, the differences are relevant not in the maximum surface values but in the curve trend. In the less dense material the plateau is reached at a greater depth than in the more dense material due to the major penetration of the nitriding agents.

The influence of treatment time can be studied by comparing treatments 1 (8 h) and 2 (24 h) (only nitriding). When the time increases there is only a slight increase in the thickness of the white layer while the diffusion zone is practically the same. The maximum microhardness value is not dramatically influenced by the increase in treatment time.

In the case of the denser material the longer treatment shifts the profile towards the centre of the sample. For material B there are no significant differences. Changes in the nitriding atmosphere cause considerable differences in the results. Treatment 3 with an higher amount of N_2 and traces of CH_4 produces a typical irregular white layer but with an average thickness higher than that for treatments 1 and 2. The white layer is composed prevalently by γ' but also ε phase is present especially in the less dense material. This is the reason for the higher microhardness values on the surface of this material. The ε phase is mainly localed at the interface between the γ' phase and the azoferrite below. However the amount of ε phase is so limited that it does not influence the hardness HV1 and HV5.

5. Conclusions

1. The ion nitriding process is also effective on less dense material while the volume mass is a discriminative factor for potential controlled gas nitriding [6]. The dimensional variations are within the applicability range ($\leq$0.12%) for the ion nitriding process while in the case of gas nitriding there was up to 1.6% of variation for material B. The ion nitriding process does not produce micropores in the white layer as the Nitreg treatment does [6].

2. The volume mass has an influence on the morphology and microstructure of the nitrided alloys. The compound layers are thinner and more irregular in the less dense material. The treatment parameters influence the microstructure of the diffusion layer. Together with the azoferrite grains the principal constituents are large amounts of needle shaped nitrides that have no effect on hardness and diffusion and precipitation phenomenon at grain boundaries [4, 6].

3. The higher surface hardness is obtained with treatment 3 with an higher N content and traces of CH_4. From the previous observations it is evident that there is little effect of the long treatment times. On the contrary it could be interesting to test shorter process times.

Acknowledgements

The authors want to acknowledge Höganas AB for supplying the samples and Professor Giordano, Department of Materials Science and Technology, Faculty of Engineering, University of Genoa, for the porosity measurements with the Hg porosimeter.

References

1. G. F. BOCCHINI, "Metallografia dei materiali sinterizzati" Corso d'aggiornamento presso la Hoganas Italia S.r.l., Rapallo 1994.
2. B. LINDQVIST, "A Molibdenum-Alloyed P/M Steel for Surface Hardening," edited by Hoganas (Hoganas AB, Sweden 1986).
3. K. S. NARASIMBAN, *Adv. Perform. Mat.* **1** (1996) 7.
4. G. PRADELLI, T. BACCI, B. TESI, A. MOLINARI and G. F. BOCCHINI, in Atti 13° Convegno Nazionale AIM sui trattamenti termici, Salsomaggiore, novembre 1992 edited by AIM, Milano, 1992, p. 123.
5. G. F. BOCCHINI, *Metal Powder Report* (1990) 772; (Febb.) (1991) 52.
6. M. R. PINASCO, M. G. IENCO, E. STAGNO, G. PALOMBARINI, G. F. BOCCHINI and M. BRUZZONE, *La Metallurgia Italiana* **86**(8/9) (1994) 411.
7. J. M. O'BRIEN and D. GOODMAN, in "ASM Handbook, Vol. 4, Heat Treating" (ASM International, Metals Park, Ohio, 1991) p. 420.
8. E. MELETIS and S. YAN, *J. Vac. Sci. Technol.* **A11**(1) (1993) 25.
9. A. LEJLAND, K. S. FANCEY and A. MATTHEWS, *Surface Engineering* **4**(3) (1991) 207.
10. W. REMGES and W. ZIMMERMANN, in Proc. Conf. PM World Congress, S. Francisco, USA, 1992, p. 321.
11. G. F. BOCCHINI, "in Proc.Conf. Quatrieme symposium europeen de metallurgie des poudres, Grenoble, 1975, p. 145.
12. P. F. COLIJN, E. J. MITTEMEIJER and H. C. F. ROZENDAAL, *Z. Metallkde* **74**(9) (1983) 620.
13. H. C. F. ROZENDAAL, P. F. COLYN and E. J. MITTEMEIJER, *Surface Engineering* **1**(1) (1985) 101.
14. M. A. J. SOMERS, P. F. COLIJN, W. G. SLOOP and E. J. MITTEMEIJER, *Z. Metallkde* **81**(1) (1990) 33.
15. G. F. BOCCHINI, A. MOLINARI, B. TESI and T. BACCI, *Metal Powder Report* **45**(11) (1990).
16. M. R. PINASCO, G. PALOMBARINI, M. G. IENCO and G. F. BOCCHINI, *Journal of Alloys and Compounds* **220** (1995) 217.

Received 7 July 1999
and accepted 18 February 2000